Metabolic Engineering 12 (2010) 187–195

Contents lists available at ScienceDirect

Metabolic Engineering

journal homepage: www.elsevier.com/locate/ymben

Analysis of polyhydroxybutyrate flux limitations by systematic genetic and metabolic perturbations

Keith E.J. Tyo, Curt R. Fischer, Fritz Simeon, Gregory Stephanopoulos *

Department of Chemical Engineering, Massachusetts Institute of Technology, Cambridge, MA 02139, USA

ARTICLE INFO

Article history:
Received 27 March 2009
Received in revised form
20 October 2009
Accepted 21 October 2009
Available online 30 October 2009

Keywords:
Poly-3-hydroxybutyrate
PHB
Chemostat
Flux control
Overexpression

ABSTRACT

Poly-3-hydroxybutyrate (PHB) titers in *Escherichia coli* have benefited from 10+ years of metabolic engineering. In the majority of studies, PHB content, expressed as percent PHB (dry cell weight), is increased, although this increase can be explained by decreases in growth rate or increases in PHB flux. In this study, growth rate and PHB flux were quantified directly in response to systematic manipulation of (1) gene expression in the product-forming pathway and (2) growth rates in a nitrogen-limited chemostat. Gene expression manipulation revealed acetoacetyl-CoA reductase (*phaB*) limits flux to PHB, although overexpression of the entire pathway pushed the flux even higher. These increases in PHB flux are accompanied by decreases in growth rate, which can be explained by carbon diversion, rather than toxic effects of the PHB pathway. In chemostats, PHB flux was insensitive to growth rate. These results imply that PHB flux is primarily controlled by the expression levels of the product forming pathway and not by the availability of precursors. These results confirm prior *in vitro* measurements and metabolic models and show expression level is a major affecter of PHB flux.

1. Introduction

Growth-associated biochemical production requires a sensitive balance between product formation (specific productivity) and biomass formation (growth rate). Given that specific substrate uptake rates are finite, resources diverted to biomass and product cannot exceed a defined rate, forcing a tradeoff between the two. While product formation is the objective of a biochemical process, increasing the flux to product will eventually inhibit growth by starving the cell for resources necessary for growth, thus reducing the rate of biocatalyst production. In addition, toxicity of accumulated products or intermediates that are a result of increased diversion of resources to the product forming pathway may also hinder growth beyond what is acceptable. From an overall productivity, a precisely defined product flux is essential to maximize yield and productivity.

A carefully defined product flux is especially true in the case of growth during poly-3-hydroxybutyrate (PHB) synthesis, where the product is expected to use a large portion of glucose uptake and may be toxic due to the large intracellular PHB granules (Anderson and Dawes, 1990), thereby potentially hindering growth rate significantly. Polyhydroxyalkanoates (PHAs), the family of polyesters that include PHB, are a possible replacement for many petrochemical-based polymers that are used today. Because PHAs use renewable resources as feedstock and are biodegradable, certain co-polymer PHAs could offer 'green' replacements for commonly used polyolefins (Anderson and Dawes, 1990). PHB production in recombinant *Escherichia coli* is attractive for a number of reasons: titers as high as 75% are possible (Wang and Lee, 1997), purification of the polymer from *E. coli* is easy, and there are no known PHB depolymerases in *E. coli* (Madison and Huisman, 1999). A continuous process may be attractive for PHB production in *E. coli* because chemostats enjoy greater utilization of installed capital, lower equipment sizes, and increased volumetric productivities (when calculated including down-times inherent in batch processes), which may be helpful for this low value product. However, for continuous production simultaneous generation of both biomass and PHB is required because only a limited amount of PHB can be stored intracellularly. To date little work has explored continuous production for PHB. Previous studies have shown that PHB accumulation primarily occurs in stationary phase and very little accumulation happens in log phase growth (Wang and Lee, 1997). These characteristics would not be amenable for growth phase accumulation, and thus new engineering strategies need to be employed to improve growth phase accumulation.

PHB specific productivity (unless otherwise specified, productivity will refer to specific productivity), or flux, can be limited by available precursors to the product-forming pathway or activity of the enzymes in the pathway. The committed PHB pathway consists of three steps that convert two acetyl-CoA moieties and

* Corresponding author. Department of Chemical Engineering, Massachusetts Institute of Technology, Room 56-469, Cambridge, MA 02139, USA.
Fax: +1 617 253 3122.
E-mail address: gregstep@mit.edu (G. Stephanopoulos).

1096-7176/$ - see front matter © 2009 Elsevier Inc. All rights reserved.
doi:10.1016/j.ymben.2009.10.005

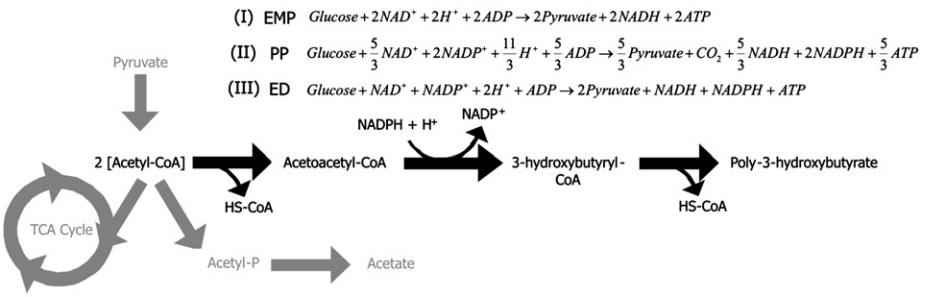

Fig. 1. Glucose metabolism to poly-3-hydroxybutyrate. Conversion of glucose to pyruvate can occur by three pathways that have different pyruvate yields and produce different reducing equivalents: (I) Embden–Meyerhof–Parnas (EMP) pathway (glycolysis), (II) pentose phosphate (PP) pathway, and (III) Entner–Doudoroff (ED) pathway. The ED pathway does not provide as much ATP, but provides the exact amount of NADPH required for PHB synthesis. [Metabolic map] The recombinant PHB pathway (black) competes for acetyl-CoA, a central node for many different biosynthesis routes, with native pathways of TCA cycle, and acetate synthesis (grey), among others. Oxidation state of the NADPH/$NADP^+$ pool and levels of acetyl phosphate may regulate the entry of acetyl-CoA to various pathways.

one reducing equivalent (NADPH) to one unit of PHB (Fig. 1). The three enzymes in the PHB pathway are β-ketothiolase, acetoacetyl-CoA reductase (AAR), and PHB synthase, encoded by the genes *phaA*, *phaB*, and *phaEC* (or *phaC*), respectively. PHB metabolized from glucose has an excess of reducing equivalents (shown as H_2) as shown in Eq. (1). The chemical reactions in Fig. 1(I–III) show that *E. coli* can metabolize glucose in a variety of ways that provide different forms of reducing cofactors and energy as byproducts while providing acetyl-CoA for PHB production.

$$n C_6H_{12}O_6 \rightarrow (C_4H_6O_2)_n + 2nCO_2 + 3nH_2 \quad (1)$$

PHB content, the most commonly reported and industrially relevant parameter, can be misleading when trying to interpret biological mechanisms. PHB content can be increased by either increasing PHB flux or retarding growth rate. Metabolic engineering schemes often have significant effects on growth rate, independent of the PHB pathway. It is possible for flux to PHB to be unchanged, while a decreased growth rate will give higher PHB accumulation. Increased PHB content is always good; however, overall productivity is best improved by perturbations that increase PHB flux directly. From an industrial standpoint, this would reduce batch times or allow for continuous operation.

The literature offers conflicting viewpoints as to what limits PHB flux. Some have implicated NADPH as a limiting reagent under growth conditions. These studies have focused on altering the redox balance in the cell through (a) phosphoglucose isomerase (*pgi*) deletion, (b) overexpression of pentose phosphate (PP) pathway enzymes (*zwf*, *gnd*, *talA*, and *tktA*), (c) gluconate feeding, or (d) transhydrogenase overexpression (Jung et al., 2004; Lim et al., 2002; Sanchez et al., 2006; Shi et al., 1999; Song et al., 2006). These act through (a) preventing glucose from being metabolized through the Embden–Meyerhof–Parnas (EMP) pathway, and instead metabolized through the PP pathway or the Entner–Doudoroff (ED) pathway, making NADPH instead of NADH, (b) increasing activity of PP pathway causing the same redirection as in (a), (c) feeding substrates naturally metabolized by the PP or ED pathways, and (d) catalyzing electron exchange from NADH to NADP+.

While the above studies did increase NADPH supply, it is unclear whether the observed increases in flux to PHB were a result of overcoming a NADPH shortage to the PHB pathway, making more acetyl-CoA available for PHB biosynthesis by downregulating other acetyl-CoA consuming reactions, or general growth retardation, which would allow a higher PHB cell content. For PHB production on glucose, measurements of NADPH/NADP+ ratio was 3 and NADPH concentration was 225 μM (van Wegen et al., 2001). This is higher than the NADPH K_m of AAR, 19 μM (Steinbuchel and Schlegel, 1991), which should be sufficient to supply NADPH. Hong et al. (2003) have shown that carbon is directed down the ED pathway to provide more NADPH for PHB production (unlike the EMP pathway, which produces NADH), implying NADPH may not be limiting. On the other hand, several pathways that consume acetyl-CoA (Fig. 1, acetyl-CoA node) are regulated in a NADPH-dependent manner. TCA cycle consumption of acetyl-CoA is linked to redox in the cell through product inhibition by NADPH of isocitrate dehydrogenase (Dean and Koshland, 1993), and allosteric inhibition by high NADPH/NADP+ ratios that have been associated with lowered citrate synthase activity for growth on glucose (Wang and Lee, 1997; Lim et al., 2002). The acetate pathway is regulated, in part, by the need to regenerate NAD^+ (Wolfe, 2005). If NADH levels are lowered by an increased diversion of reducing equivalents to NADPH, the flux to acetate may be downregulated. In aggregate, NADPH-directed perturbations may also increase availability of acetyl-CoA for the PHB pathway by NADPH-induced downregulation of competing pathways.

Attempts to directly improve the supply of acetyl-CoA may also have unexpected effects that further confuse experimental observations. Acetate secretion is observed in PHB producing *E. coli* under aerobic conditions (Sanchez et al., 2006), implying an excess of acetyl-CoA is available. Phosphate acetyltransferase (*pta*) and acetate kinase (*ack*) deletions, which should decrease acetate production, have also decreased PHB accumulation, implying that enzyme competition for the acetyl-CoA pool may not be the determining factor (Shi et al., 1999). Instead, the presence of acetyl phosphate may be required in order to activate PHB synthase (Miyake et al., 2000) and without acetyl phosphate the PHB pathway may thus be downregulated. Shi et al. (1999) also showed that addition of α-methyl-glucoside, a glucose analog that retards glucose uptake through non-toxic competitive inhibition, decreases acid secretion, but does not change PHB accumulation. PHB flux appears insensitive to glucose uptake, implying the pathway activity may exert metabolic control over the flux from acetyl-CoA to PHB.

The previous work has resulted in impressive PHB titers in late stationary phase (see the review by Madison and Huisman (1999) for many examples). It may be possible to shorten the batch time necessary to achieve these high titers by analyzing the rates of production, i.e. PHB flux. Pathway enzyme activities have been implicated as a possible flux limitation. *In vitro* measurements of PHB pathway enzyme activities and kinetic models have predicted that PHB flux is limited by enzyme activity, not precursor supply (Sim et al., 1997; van Wegen et al., 2001), but to date, no systematic, *in vivo* study has been undertaken to this end. In this work, we examined the effects of stepwise overexpression of the PHB pathway genes on pathway flux. Separately, the growth rate was varied through dilution rate in a nitrogen-limited chemostat

to vary biomass demand for acetyl-CoA. These experiments show that activity of the PHB pathway primarily controls the PHB flux, and careful tuning of that pathway activity is required for optimal product/biomass formation ratio.

2. Materials and methods

2.1. Strains, plasmids, primers, and media

Strains and plasmids used in this study are listed in Table 1. pAGL20, a modified pJOE7 kindly provided by Anthony Sinskey, contains the genes *phaAB* from *Ralstonia eutropha*, encoding β-ketothiolase and acetoacetyl coenzyme-A reductase, and *phaEC* from *Allochromatium vinosum*, encoding the two-subunit PHB polymerase on a kanamycin resistant backbone (Lawrence et al., 2005). pZE21 is a ColE1 plasmid with kanamycin resistance and green fluorescent protein (*gfp*) driven by a P_L-tetO promoter (Lutz and Bujard, 1997).

Cloning was performed using standard techniques and materials from New England Biosciences (Beverly, MA), and all cloning steps were performed in DH5α (Invitrogen). Table 2 lists all primers used for PCR. pZE21 was digested SacI/AatII and ligated to a chloremphenical acetyl transferase PCR product from pAC184 bearing the same sites to create pZE-Cm. Promoterless PCR products of *phaA*, *phaB*, *phaEC*, and *phaECAB* were generated from pAGL20 and cloned into the KpnI/MluI sites of pZE-Cm for the systematic overexpression study. These plasmids were co-transformed with pAGL20 into XL-1 Blue and characterized. Whole operon promoter replacement was accomplished by synthesizing the tac promoter from oligonucleotides and cloning into the AatII/EcoRI site of pZE21. A promoterless *phaECAB* PCR product from pAGL20 was then cloned into the KpnI/MluI sites. This plasmid was transformed into XL-1 Blue and characterized.

K12 *recA::kan* TGD(cat+PHB) was created using tandem gene duplication, and contains 25 copies of the *phaECAB* operon integrated in tandem on the *E. coli* genome at the *attB* phage integration site (Tyo et al., 2009). This strain was used for the chemostat studies because of the improved genetic stability over plasmid-based expression systems.

Strains were cultured in the minimal media, MR with 20 g/L glucose (for shake flasks) or 30 g/L glucose (for chemostats) at 37 °C (called MR from here onward). MR medium was prepared as defined previously (Wang and Lee, 1997). Luria–Bertani (LB) broth was used for growth on solid media and standard preparations of cells. Biomass is reported as residual cell weight (RCW), the non-PHB fraction of the cell pellet.

2.2. Systematic overexpression studies

XL1-Blue was transformed with the prescribed plasmid(s). Colonies were picked and grown in a 14 mL culture tube with 5 mL of LB for 12 h. 0.5 mL of the culture was inoculated into a 14 mL culture tube with 5 mL MR and cultured for 12 h. Cells were then inoculated into a 250 mL Erlenmeyer flask with a working volume of 50 mL MR+20 g/L glucose+10 mg/L thiamine to a starting A_{600}=0.015. Cultures were grown to log phase and harvested at A_{600}=2.0–2.5. Prior experiments showed cells were at steady state, exponential growth at this point in the cell culture (data not shown). Growth rate, percent PHB (dry cell weight—DCW), and transcriptional measurements were taken as described below. Specific PHB productivity was estimated as the product of specific growth rate and percent PHB (DCW), which is exact at the limit of steady state growth. 34 μg/mL chloramphenicol and/or 25 μg/mL kanamycin was used to maintain plasmids in each experiment.

2.3. Chemostats

Nitrogen-limited chemostat experiments were performed in a 3 L stirred glass vessel using the BioFlo 110 modular fermentation system (New Brunswick Scientific, Edison, NJ) with a 1 L working volume. Bioreactor controllers were set to pH=6.9, adjusted by 6 N NaOH through controller, 30% dissolved oxygen, controlled by adjusting feed oxygen concentration, and temperature at 37 °C, controlled by a thermal blanket and cooling coil. Gas flow was set at 3 L/min and agitation at 400 rpm. Antifoam SE-15 (Sigma-Aldrich, St. Louis, MO) was diluted in water and added by peristaltic pump to control foaming.

Sterile MR media+30 g/L glucose without antibiotics was fed by peristaltic pump at flowrates of 50, 100, and 300 mL/h and culture broth was removed from the reactor using a level-stat. 10 mL samples were taken for characterization after four residence times at a given flowrate. Approach to steady state was verified by glucose concentration in the reactor. Three measurements, each spaced one residence time apart, were taken at each steady state. Ammonium, the only nitrogen source, was monitored semi-quantitatively by NH_4^+ test strips (Merck KGaA, Darmstadt, Germany), and was always below 10 mg/L. Duplicate chemostats were run. Contamination was checked by streaking

Table 1
Strains and plasmids used in this study.

Name	Description	Reference
Strains		
XL1-Blue	Cloning/expression strain of *E. coli*	Stratagene (La Jolla, Calif.)
K12 recA::kan TGD (cat+PHB)	25 tandem copies of PHB biosynthetic operon from pAGL20 on *E. coli* genome	(Tyo et al., 2009)
Plasmids		
pAGL20	PHB biosynthetic pathway on modified pJOE7	(Lawrence et al., 2005)
pZE21	Medium copy plasmid (ColE1 origin, kan^R)	(Lutz and Bujard, 1997)
pZE-Cm	pZE21 with kan^R replaced with Cm^R	This study
pZE-phaA	pZE derivative with cat and R. eutrophus phaA	This study
pZE-phaB	pZE derivative with cat and R. eutrophus phaB	This study
pZE-phaEC	pZE derivative with cat and R. eutrophus phaA	This study
pZE-gfp	pZE derivative with cat and gfp	This study
pZE-phaECAB	pZE derivative with cat and pAGL20 PHB operon	This study
pZE-tac-phaECAB	pZE derivative with pAGL20 PHB operon driven by strong promoter (P_{tac})	This study

Table 2
Oligonucleotides and their sequences used in this study.

Name	Restriction site	Sequence (5′-3′)
Cm (s)	AatII	AAA**GACGTC**CGTTGATCGGCACGTAAGAGGTTCC
Cm (a)	SacI	AA**GAGCTC**CCTTAAAAAAATTACGCCCCGCCC
phaA (s)	KpnI	GG**GGTACC**GCATGACTGACGTTGTCATCGTATCCGC
phaA (a)	MluI	CG**ACGCGT**CGGAAAACCCCTTCCTTATTTGCG
phaB (s)	KpnI	GG**GGTACC**GCATGACTCAGCGCATTGCGTATGTGAC
phaB (a)	MluI	CG**ACGCGT**CCGACTGGTTGAACCAGGCCG
phaEC (s)	KpnI	GG**GGTACC**GACGGCAGAGAGACAATCAAATCATG
phaEC (a)	MluI	CG**ACGCGT**ATGGAAACGGGAGGGAACCTGC
tac promoter (s)		GAGCTGTTGACAATTAATCATCGGCTCGTATAATGTGTGG
tac promoter (a)	AatII/EcoRI	**AATT**CCACACATTATACGAGCCGATGATTAATTGTCAACAGCTC**ACGT**
qPCR phaA (s)		CGTTGTCATCGTATCCGCCG
qPCR phaA (a)		GACTTCGCTCACCTGCTCCG
qPCR phaB (s)		GTGGTGTTCCGCAAGATGAC
qPCR phaB (a)		CGTTCACCGACGAGATGTTG
qPCR phaE (s)		GGAGCAGAGCCAGTATCAGG
qPCR phaE (a)		CACCCTGGATGTAGGAGCCC
qPCR rrsA (s)		AGGCCTTCGGGTTGTAAAGT
qPCR rrsA (a)		ATTCCGATTAACGCTTGCAC

broth on nile red/LB plates and checking that all colonies were PHB^+ by nile red fluorescence (Spiekermann et al., 1999).

2.4. Analytical methods

Cell densities were monitored at 600 nm using an Ulstrapec 2100pro (Amersham Biosciences, Uppsala, Sweden). Cell and PHB concentrations were determined as previously described (Tyo et al., 2006). Glucose concentrations were measured by a glucose analyzer (Yellow Springs Instruments, Yellow Springs, OH). Acetate was measured by high-pressure liquid chromatography using an Aminex HPX-87H ion-exclusion column (300 7.8 mm; Bio-Rad, Hercules, CA) and 14 mM H_2SO_4 mobile phase at 50 °C and 0.7 mL/min. Cell culture supernatant was kept at −20 °C before analysis.

2.5. Transcriptional analysis

RNA was isolated from growing cells at A_{600}=2.0 using the RNEasy Protect Bacteria mini kit (Qiagen USA, Valencia, CA), according to the manufacturer's protocol, and diluted to 20 ng/μL total RNA; 60 ng isolated RNA was converted to cDNA using the ImpromII reverse transcriptase (Promega, Madison, WI) with 1 μg random hexamers according to the manufacturer's protocol. cDNA concentrations of *phaA*, *phaB*, *phaE*, and *rrsA* were determined by qPCR using a Biorad iCycler and the iQ SYBR Green Supermix (Biorad) using 5 μL of a 100-fold dilution of the cDNA reaction for the *pha* and *rrsA* genes, according to the manufacturer's protocol. qPCR primers are shown in Table 2. A standard curve for *pha* genes was made using dilutions of pAGL20, cut once to relax supercoiling. *rrsA* standard curve was generated using a purified PCR product of the genomic rrsA. Relative expression was computed by normalizing each *pha* gene by the housekeeping gene *rrsA*. Controls without reverse transcriptase were used to verify that contaminating DNA was negligible.

2.6. Flux balance analysis

Flux balance analysis was done with a previously existing stoichiometric model (Edwards and Palsson, 2000), supplemented with three metabolic reactions and one exchange flux that together allow for PHB synthesis from acetyl-CoA: (i) 2 AcCoA→AcAcCoA+CoASH; (ii) AcAcCoA+NADPH→3HBCoA+NADP; and (iii) 3HBCoA→PHB+CoASH. The exchange flux was PHB→∅, representing the net formation and export of PHB from the metabolically active portion of the cytoplasm.

The stoichiometric trade-off between growth yield and PHB yield (on glucose) was calculated as described by Bell and Palsson (2005, Introduction). Briefly, the PHB yield was constrained to a certain value *s*, and then the biomass yield was maximized subject to the usual FBA constraints as well as the PHB constraint. By repeating the optimization at varying values of *s*, we obtained the full projection, in the two dimensions of PHB yield and biomass yield, of the feasible region of flux space.

Calculations were done with MATLAB software (The Mathworks, Natick, MA), and the TOMLAB interface (Tomlab Optimization, Inc., Trefasgatan, Sweden) to the linear program solver CPLEX 9.0 (ILOG, Gentilly, France).

Biomass and PHB yields calculated from the model were converted to specific productivities (of growth and PHB, respectively), by multiplying by the specific glucose uptake rate. Glucose consumption was measured at 1.1 g glucose/(gRCW-h), yielding a maximal growth rate (from stoichiometric model) of 0.57 h^{-1} and a maximal PHB production rate of 530 mg PHB/(gRCW-h).

3. Results

3.1. Systematic overexpression of PHB pathway

A convenient assay for studying the relationship between PHB flux and maximal growth rate was devised in exponentially growing cells. At steady state, PHB content, specific growth rate, and PHB flux can be quantified. Under these conditions, PHB content (%PHB (DCW)) is significantly less than in late stationary phase, which is typically characterized.

The sensitivity of PHB flux to perturbations in PHB pathway gene expression levels was analyzed by sequential overexpression of the *phaA*, *phaB*, and *phaEC* genes from the pZE-Cm plasmid in the background of a second plasmid (pAGL20) that expressed the entire PHB operon from the native *R. eutropha* promoter. We hypothesized that the flux control would lie in the activity of the product forming pathway enzymes and not in the precursor availability (acetyl-CoA or NADPH) during growth on glucose.

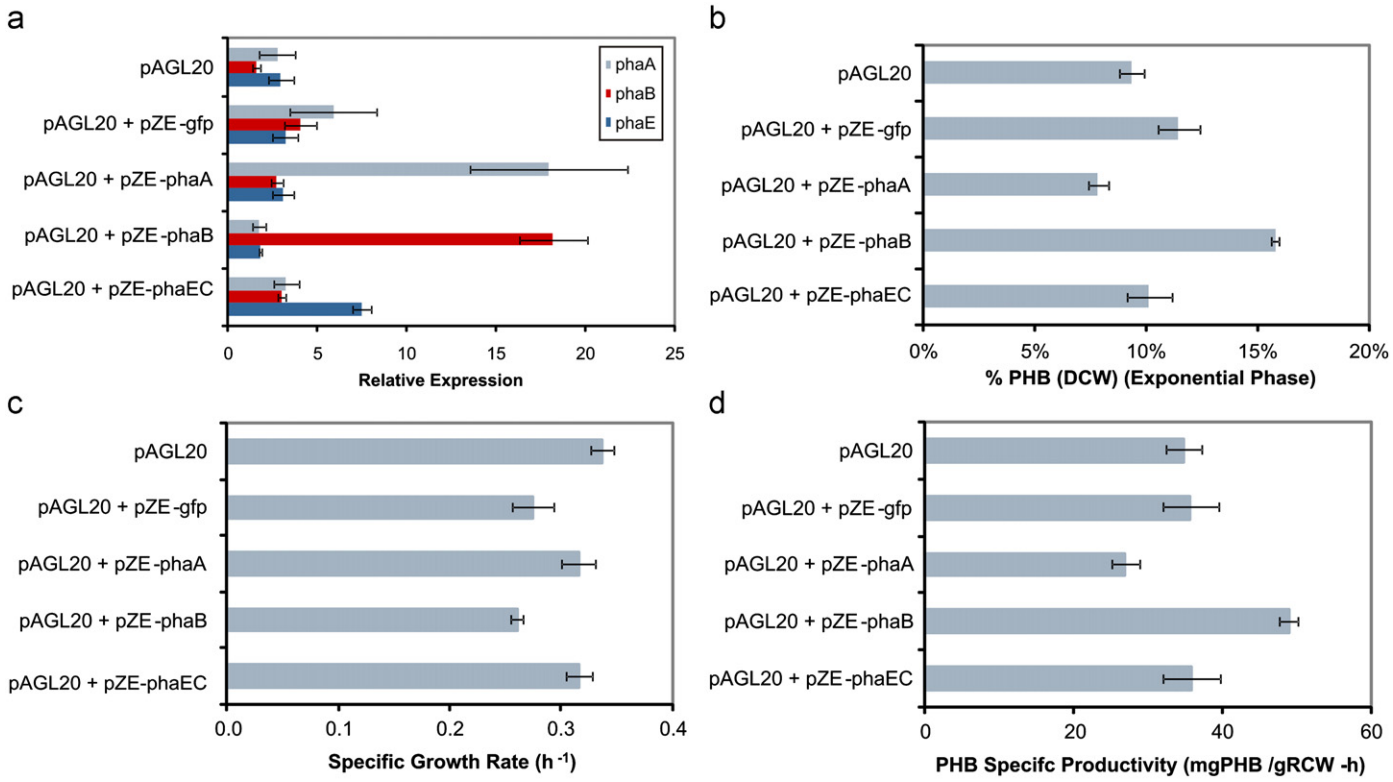

Fig. 2. Systematic overexpression of steps in PHB pathway. *phaA*, *phaB*, *phaEC*, and *gfp* were overexpressed in the presence of a second plasmid containing the complete PHB operon. Strains were characterized in the exponential phase. (a) Relative RNA levels normalized to *rrsA*. (b) Exponential phase PHB accumulation. (c) Specific growth rates. (d) Specific PHB productivity. DCW—dry cell weight, total biomass fraction (RCW+PHB), RCW—residual cell weight, non-PHB fraction of biomass. Error bars are s.e.m. $n=4$ for RNA and s.e.m. $n=3$ for other measurements.

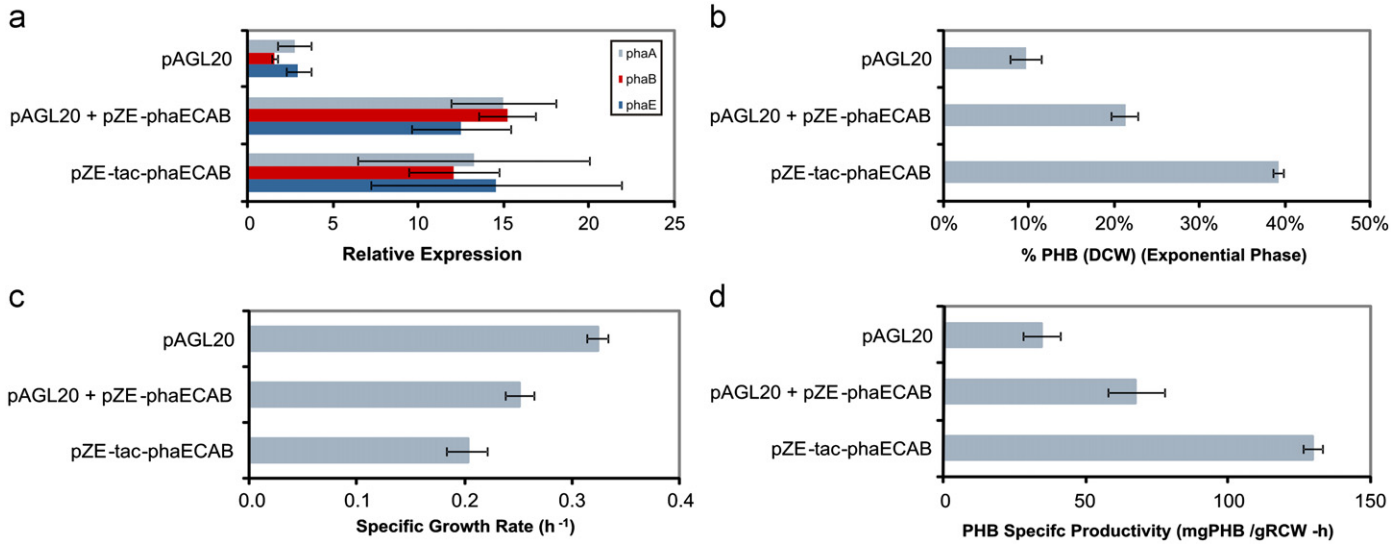

Fig. 3. Overexpression of the entire PHB pathway. The PHB operon was expressed by one or two plasmids with different promoters. Strains were characterized in the exponential phase. (a) Relative RNA levels normalized to *rrsA*. (b) Exponential phase PHB accumulation. (c) Specific growth rates. (d) Specific PHB productivity. DCW—dry cell weight, total biomass fraction (RCW+PHB), RCW—residual cell weight, non-PHB fraction of biomass. Error bars are s.e.m.; $n=4$ for RNA and s.e.m. $n=3$ for other measurements.

Quantitative RT-PCR was used to verify perturbations in expression, and growth and PHB properties were measured in the exponential phase. Fig. 2 shows the increase in transcript levels and the corresponding phenotypic change in PHB production for each of the three overexpressions compared to the controls. GFP overexpression was included to control for additional burden to the cell by a plasmid/gene product unrelated to PHB. Fig. 2(a) shows the transcript levels were increased by 2–11 fold for each of the three genes. *phaB* was found to exert the most flux control over the system and increased the PHB flux by 37% (Fig. 2(d)). The

other two steps in the pathway, *phaA* and *phaEC*, do not increase the flux to PHB on overexpression, and therefore do not exhibit flux control over the pathway. While GFP did increase the PHB content (Fig. 2(b)), the flux remained unchanged (Fig. 2(d)). This is primarily due to a decrease in growth rate (Fig. 2(c)), thereby decreasing 'dilution by growth' and increasing PHB content for the same flux. The maximal specific growth rate was inversely related to the PHB flux (Fig. 2(c)), as might be expected by either (1) an increased diversion of carbon from biomass to PHB or (2) PHB toxicity, due to more and/or larger granules of PHB accumulating in the cytoplasm, as seen in the PHB accumulation (Fig. 2(b)). However, the negative effect on growth rate is rather small. This interplay between PHB flux and specific growth rate will be analyzed in more detail below.

Next, the expression of the entire PHB operon was increased by either (1) expressing the operon from two plasmids (pAGL20+pZE-phaECAB) or (2) changing the promoter from P_{LtetO1} to the stronger promoter, P_{tac} (pZE-tac-phaECAB). This revealed further increase in flux was possible. Fig. 3 shows the transcriptional and phenotypic effects of overexpressing the entire operon. While *phaB* overexpression removed the AAR limitation, by overexpressing all three genes, additional limitations were overcome, resulting in flux increases of 170% beyond the PHB flux with *phaB* overexpression (270% above pAGL20). While both pAGL20+pZE-phaECAB and pZE-tac-phaECAB had similar expression levels, the highest PHB flux was obtained with only one plasmid using a strong P_{tac} promoter. This is presumably due to the additional carbon and energy requirements involved in replicating a second plasmid that reduced PHB productivity. A comparison of stationary phase PHB production in shake flask showed that the pZE-tac-phaECAB strain accumulated product to 69.9% PHB (DCW)[+/−0.4% s.e.m.] in 31 h compared to 38.8% PHB (DCW)[+/−0.1% s.e.m.] in 45 h. PHB content reached levels found in controlled fermentors, although the batch cycle is notably shorter (Wang and Lee, 1997).

As before, increases in PHB flux were correlated with decreases in growth rate. This was specifically true for other promoters (P_{T5}, P_{rrnB}) that are stronger than P_{tac} (data not shown). When inoculated in MR medium, strains with very strong promoters grew extremely slow (growth rates of $\sim 0.03\,h^{-1}$) and were genetically unstable: cells defective in PHB production overtook the culture after a long lag phase (data not shown). While genetic instabilities made these strains impossible to characterize, it is suspected that PHB productivities exceeded a threshold beyond which resource consumption or toxicity due to large PHB granules reduced growth to almost nothing. This represents a regime of PHB pathway expression where the PHB/biomass ratio has become too high and is prohibitively toxic to the cell.

3.2. PHB production in nitrogen-limited chemostat

Nitrogen-limited chemostats allow growth rates to be varied independently by controlling the dilution rate under aerobic, nitrogen-limiting conditions and measuring the effect of growth rate variation on PHB flux. In contrast to the overexpression experiments, where the expression of PHB pathway genes were changed and the cells were allowed to grow at their maximal growth rate, here the growth rate was changed, while the PHB pathway genetics were held constant. Excess glucose should ensure substrate is available at all times. To this end, the tandem integrated PHB operon strain, K12 *recA*::*kan* TGD (cat+PHB), was grown at steady state in nitrogen-limited chemostats at different dilution rates. Table 3 shows measured parameters of the culture at three dilution rates. Fig. 4 shows the fluxes of glucose uptake and biomass, PHB, and acetate formation on a C-mol basis for ease of comparison. C-mol fluxes were determined by direct measurement of each metabolite/biomass in the chemostat and known or measured C-mol yields for each from glucose.

An excess of glucose (under nitrogen-limiting conditions) provided an abundant substrate supply for PHB accumulation, although at the lowest dilution rate, the glucose concentration was reduced to 0.3 g/L. This is presumably due to the dominance of maintenance requirements in the cell at low growth rates. Biomass concentration was nearly constant across all dilution rates as would be expected for nitrogen-limited growth and was set by the concentration of nitrogen in the feed (and the biomass yield of *E. coli* on ammonium). It can be noted that the increasing trend of biomass concentrations with increasing dilution rates is contrary to what might be expected from the chemostat theory, however, the differences, overall, are not significant. Changes in specific glucose uptake were accounted for by the change in glucose demand for biomass as seen by the parallel lines of biomass and total glucose consumed in Fig. 4. Although the amount of PHB decreased in the reactor with increasing dilution rate, the PHB yield and PHB flux remained relatively constant.

Table 3
PHB production in chemostat*.

Dilution rate		$0.05\,h^{-1}$	$0.10\,h^{-1}$	$0.30\,h^{-1}$
% PHB (DCW)		49	37	22
Yield (g PHB/g GLU)		0.098	0.094	0.080
% of Theoretical Max Yield		20	20	17
Concentrations** (g/L)	X	3.08	3.30	3.48
	PHB	2.9	2.0	1.0
	ACE	2.5+/−0.50	2.5	1.1
	GLU	0.3+/−0.27	9.1	17.8
Volumetric Productivities (g/(L h))	X	0.15	0.33	1.04
	PHB	0.15	0.20	0.29
	ACE	0.13+/−0.03	0.25	0.32
	GLU	1.48	2.09	3.66
Specific Productivities (g/(g biomass h))	X	0.05+/−0.003	0.10	0.30
	PHB	0.05+/−0.003	0.06	0.08
	ACE	0.04+/−0.008	0.08	0.09
	GLU	0.48	0.63	1.05

X – biomass; PHB – poly-3-hydroxybutyrate; ACE – acetate; GLU – glucose.
*Coefficient of variation $<5\%$ for all measurements unless noted.
**Feed concentrations were 30 g/L GLU. No X, PHB, or ACE were present in the feed.

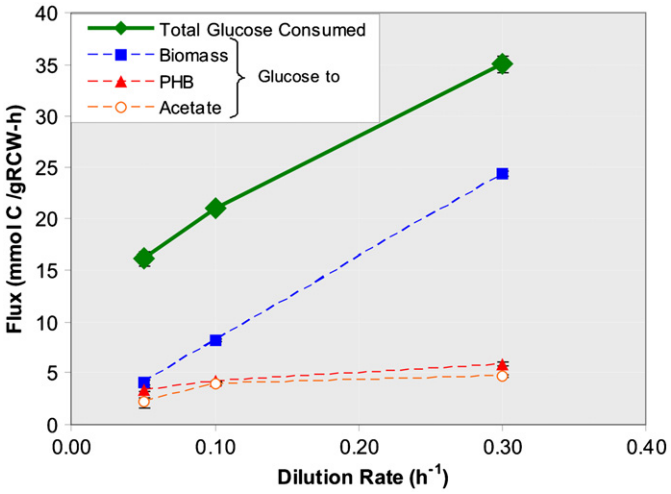

Fig. 4. C-mol fluxes in PHB nitrogen-limited chemostat. K12 *recA*::*kan* TGD(*cat+PHB*) was grown in a nitrogen-limited chemostat. Steady state rates of metabolite formation/consumption were measured and converted to C-mols. Glucose consumed for biomass (non-PHB), PHB, and acetate was based on assumed yields. Assumed yields on glucose; biomass—0.41 g/g, PHB—0.48 g/g, acetate—0.66 g/g. Calculated as:

$$q_{\text{glucose}} = \frac{D(C^{\text{feed}}_{\text{glucose}} - C^{\text{residual}}_{\text{glucose}})}{C_{\text{biomass}}}\left(\frac{6\,\text{mmol C}}{0.181\,\text{g glucose}}\right)$$

$$q_{\text{others}} = \frac{D(C^{\text{feed}}_{\text{others}} - C^{\text{residual}}_{\text{others}})}{C_{\text{biomass}}}\left(\frac{1}{Y_{\text{other/glucose}}}\right)\left(\frac{6\,\text{mmol C}}{0.181\,\text{g glucose}}\right)$$

PHB specific productivity did increase by a factor of 1.6 for the six-fold change in growth rate; however, this was the least change of all rates measured. Actually, the small PHB increase was in the opposite direction than would be expected for slowing growth. Acetate production was present, consuming as much glucose as PHB, and was also insensitive to the dilution rate, even though dissolved oxygen was kept above 30% throughout the experiment. High acetate production is expected with excess glucose (Wolfe, 2005).

3.3. Comparison of experimental observations to a stoichiometric maximal model

To better understand the observed trade-offs between growth and PHB production, the PHB/growth data gathered from the overexpression study and chemostat were compared to the results of a stoichiometric model of *E. coli* metabolism. Fig. 5 shows the data from the overexpression and chemostat studies overlaid with stoichiometric envelope constraining the relationship between the flux to PHB and the flux to growth. The envelope was based on a genome-scale metabolic network model of *E. coli* metabolism (Edwards and Palsson, 2000) modified to include the PHB reactions.

In the overexpression study, pathway expression was changed but cell growth was unconstrained. That is, each strain grew in batch culture at its strain-specific maximum growth rate. The trend in the overexpression experimental data shows a tradeoff between product formation and growth, which is broadly similar to the predictions of the stoichiometric model. The overexpression data fall well to the left of the stoichiometrically optimal growth rate envelope. Part of the reason for this discrepancy is *E. coli* K12's well known acetate overflow metabolism, which allows

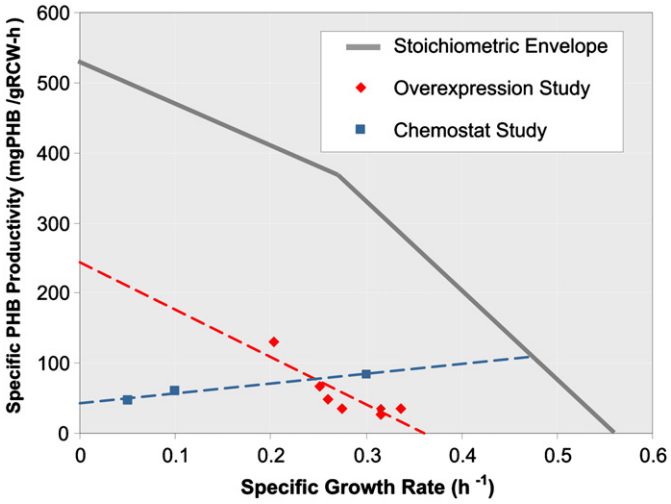

Fig. 5. Comparison of overexpression and chemostat study to stoichiometric model for PHB in *E. coli*. PHB specific productivities and specific growth rates from overexpression and chemostat studies are compared to the maximal stoichiometric trade-off. Solid line represents an *E. coli* stoichiometric model (see text). Stoichiometric model was used to predict the biomass yield at different PHB yields. Data points for overexpression and chemostat studies are for all perturbations attempted. Dashed lines are a best fit for each of the two sets of perturbations.

faster growth at high glucose concentrations, at the penalty of stoichiometrically submaximal biomass yields (Wolfe, 2005). Another reason may be the use of an XL-1 Blue background strain in this study, as opposed to the wild-type K12 for which the stoichiometric model was developed.

However, the observed trade-off between PHB flux and cell growth was close to stoichiometrically optimal, as parameterized by slopes of lines from the overexpression study and stoichiometric model in Fig. 5. Under the low-growth segment of the stoichiometric envelope, the stoichiometrically optimal trade-off between PHB and biomass was 610 mg PHB/gDCW. The slope of the high-growth segment was ~1280 mg PHB/gDCW. The best-fit line through the overexpression data showed that the observed trade-off was approximately 680 mg PHB/gDCW. In contrast, PHB flux in the nitrogen-limited chemostat was relatively invariant, with respect to changes in growth rate. As growth rates decreased, *E. coli* was unable to direct surplus glucose available in the chemostat environment toward PHB production, although it should be feasible in the stoichiometric space calculated.

4. Discussion

This study focused on the interaction between pathway enzyme expression levels and growth rate, and their effect on PHB flux. Prior to our pathway overexpression study, combinatorial PHB screening studies, which attempted to increase PHB productivity by introducing random genetic diversity and isolating improved PHB mutants, were unsuccessful in finding improved mutants that could be linked to genetic changes in the library (unpublished). The genetic diversity introduced in these libraries would be expected to perturb the global metabolic and regulatory network and would most likely produce improved mutants by increasing the supply of precursors (acetyl-CoA or NADPH). Because no mutants could be found that improved PHB productivity, it was hypothesized that limitations in the product-forming pathway (which would not be expected to be perturbed in the libraries) may control the rate of PHB formation.

Indeed, PHB flux was found to be very sensitive to the level of expression of PHB pathway genes, and in particular to AAR (*phaB*). Previously, *in vitro* activities of *phaA*, *phaB*, and *phaC* were measured as 2–12, 0.033, and 1–2 units/mg total protein, respectively (Wang and Lee, 1997; Sim et al., 1997). Likewise, a kinetic model of the PHB pathway calculated flux control coefficients (FCCs) for *phaA*, *phaB*, and *phaC* as 0.15, 0.6, and 0.25, respectively (van Wegen et al., 2001). Our *in vivo* measurements experimentally confirm that *phaB* is indeed the controlling enzyme of the PHB pathway. Simultaneous overexpression of the entire PHB operon led to much higher PHB fluxes, likely because another step began to limit flux. The promoters P_{T5} and P_{rrnB}, which should have higher promoter strength than those examined in Fig. 3, stopped cell growth on glucose (data not shown). This observation would indicate that when PHB flux is high enough to bring the acetyl-CoA and/or NADPH concentrations to below the K_m for the PHB pathway, the levels of these metabolites are already below the requirements for cellular functions to behave normally, or else intracellular PHB granules have begun to strongly interfere with cellular processes. These results show that PHB flux can be manipulated over a broad range of fluxes by only manipulating the expression of the product-forming pathway, and that precursor shortages become limiting only when cellular function is inhibited by loss of essential intermediates.

These observations are consistent with the low *in vitro* AAR activities observed in previous studies (Sim et al., 1997; van Wegen et al., 2001). In our experiments, as in most studies, PHB is expressed in medium/high copy (+25) from plasmids or tandem genes. AAR activities in *R. eutrophus* have been reported at 0.2–0.3 U/mg total protein (Park and Lee, 1996), while AAR activities in *E. coli* are much less at 0.05 U/mg total protein (Wang and Lee, 1997). This five-fold change in activity may be the result of problems in the expression or activity of AAR. Additionally, PHB synthase has been shown to be regulated by acetyl phosphate levels, and may be repressed under conditions in *E. coli* (Kessler and Witholt, 2001). This agrees with the acetate production observed in the chemostat. Diverting carbon from acetate to PHB would increase PHB yield but may require protein engineering of the PHB synthase to deregulate allosteric effects that inhibit its activity, such as acetyl phosphate regulation.

PHB flux reveals metabolic changes more clearly than PHB accumulation. This was seen in the GFP control in Fig. 2, and PHB accumulation and flux in Table 3. In both cases the PHB specific productivity (flux) was constant, although percent PHB (% DCW) varied due to changes in growth rate. These apparent changes in PHB accumulation can convolute the metabolic analysis and complicate conclusions. In previous studies, this convolution due to changes in growth or specific PHB productivity could make analysis difficult.

Comparison of experimental data to the FBA model can lead to some useful inferences. The overexpression study, where strains were allowed to grow at their maximal growth rate, shows increased PHB flux decreases cell growth rate. Comparing these measured changes to a stoicheometrically optimal model allows us to infer the PHB pathway is not hindering growth rate in a non-specific way, such as granule toxicity (PHB content was $<20\%$ PHB (DCW) in the conditions measured). Rather, under these conditions, decreased growth can be explained by carbon diversion to PHB, as shown by the parallel lines between the overexpression data and model. In contrast, the nitrogen-limited chemostat did not vary PHB flux significantly for large changes in growth rate. It is reasonable to expect that specific glucose uptake rates would remain relatively unchanged with dilution rate, allowing glucose previously required for biomass formation to be diverted to PHB, resulting in an increased PHB flux. Surprisingly, the chemostat data did not support our hypothesis and instead revealed a flat relationship between PHB productivity and growth rate. This fact suggests that glucose uptake was regulated, even under nitrogen limitation, such that acetyl-CoA pool sizes were approximately constant regardless of growth rate or glucose availability.

Understanding that flux control is primarily in the product-forming pathway allows engineers to have a great deal of control over PHB productivity by controlling expression levels of the PHB pathway. For batch production, expression systems that suppress PHB production during growth phase and turn it on to a high level in stationary phase would be the most effective, by completely separating biocatalyst formation from product formation. Increases in flux should also decrease batch time, improving overall productivity. Continuous production could either take place as two chemostats in series with the first generating the biocatalyst and the second producing the product (analogous to the batch process), or as a single chemostat where the biocatalyst and product are produced simultaneously. In the latter case, a precisely tuned expression level would be required to maintain a PHB/biomass ratio that maximizes total productivity. As observed, an upper limit of expression exists where too much carbon is diverted to PHB yielding, on one hand a high PHB/biomass ratio, but causing very low cell viability and growth at the same time. It is important to note that altering the expression of the PHB synthase has been shown to have an effect on the quality of the PHB, specifically the molecular weight of PHB (Sim et al., 1997). In this study we have focused on the flux to the PHB pathway and the quantity of PHB. For commercial production, appropriate expression of the PHB synthase will be determined by the desired MW.

Taken together, systematic perturbation studies of gene expression and growth rate combined with PHB flux measurement have identified *in vivo* that *phaB* expression is limiting in the PHB pathway of *E. coli*. Beyond this, we have identified that pathway expression primarily controls PHB flux, rather than other pleiotropic effects, which may affect growth rate. The increases in specific productivity may be useful to improve batch times in well-studied batch processes, as well as open up opportunities for continuous processes.

Acknowledgments

We would like to acknowledge NSF Grant CBET-0730238, to Parayil Ajikumar for assistance in bioreactor setup, and Anthony Sinskey for the PHB plasmid.

References

Anderson, A.J., Dawes, E.A., 1990. Occurrence, metabolism, metabolic role, and industrial uses of bacterial polyhydroxyalkanoates. Microbiol. Rev. 54, 450–472.

Bell, S.L., Palsson, B.R., 2005. Phenotype phase plane analysis using interior point methods. Comput. Chem. Eng. 29, 481–486.

Dean, A.M., Koshland Jr, D.E., 1993. Kinetic mechanism of *Escherichia coli* isocitrate dehydrogenase. Biochemistry 32, 9302–9309.

Edwards, J.S., Palsson, B.O., 2000. The *Escherichia coli* MG1655 in silico metabolic genotype: its definition, characteristics, and capabilities. Proc. Natl. Acad. Sci. USA 97, 5528–5533.

Hong, S.H., Park, S.J., Moon, S.Y., Park, J.P., Lee, S.Y., 2003. In silico prediction and validation of the importance of the Entner–Doudoroff pathway in poly(3-hydroxybutyrate) production by metabolically engineered *Escherichia coli*. Biotechnol. Bioeng. 83, 854–863.

Jung, Y.M., Lee, J.N., Shin, H.D., Lee, Y.H., 2004. Role of tktA4 gene in pentose phosphate pathway on odd-ball biosynthesis of poly-beta-hydroxybutyrate in transformant *Escherichia coli* harboring phbCAB operon. J. Biosci. Bioeng. 98, 224–227.

Kessler, B., Witholt, B., 2001. Factors involved in the regulatory network of polyhydroxyalkanoate metabolism. J. Biotechnol. 86, 97–104.

Lawrence, A.G., Choi, J., Rha, C., Stubbe, J., Sinskey, A.J., 2005. *In vitro* analysis of the chain termination reaction in the synthesis of poly-(r)-beta-hydroxybutyrate by the class III synthase from *Allochromatium vinosum*. Biomacromolecules 6, 2113–2119.

Lim, S.J., Jung, Y.M., Shin, H.D., Lee, Y.H., 2002. Amplification of the NADPH-related genes zwf and gnd for the oddball biosynthesis of PHB in an *E-coli* transformant harboring a cloned phbCAB operon. J. Biosci. Bioeng. 93, 543–549.

Lutz, R., Bujard, H., 1997. Independent and tight regulation of transcriptional units in *Escherichia coli* via the LacR/O, the TetR/O and AraC/I1-I2 regulatory elements. Nucl. Acids Res. 25, 1203–1210.

Madison, L.L., Huisman, G.W., 1999. Metabolic engineering of poly(3-hydroxyalkanoates): from DNA to plastic. Microbiol. Mol. Biol. Rev. 63, 21–53.

Miyake, M., Schnackenberg, J., Kurane, R., Asada, Y., 2000. Phosphotransacetylase as a key factor in biological production of polyhydroxybutyrate. Appl. Biochem. Biotechnol. 84, 1039–1044.

Park, J.S., Lee, Y.H., 1996. Metabolic characteristics of isocitrate dehydrogenase leaky mutant of Alcaligenes eutrophus and its utilization for poly-ß-hydroxybutyrate production. J. Ferment. Bioeng. 81, 197–205.

Sanchez, A.M., Andrews, J., Hussein, I., Bennett, G.N., San, K.Y., 2006. Effect of overexpression of a soluble pyridine nucleotide transhydrogenase (UdhA) on the production of poly(3-hydroxybutyrate) in *Escherichia coli*. Biotechnol. Prog. 22, 420–425.

Shi, H., Nikawa, J., Shimizu, K., 1999. Effect of modifying metabolic network on poly-3-hydroxybutyrate biosynthesis in recombinant *Escherichia coli*. J. Biosci. Bioeng. 87, 666–677.

Sim, S.J., Snell, K.D., Hogan, S.A., Stubbe, J., Rha, C.K., Sinskey, A.J., 1997. PHA synthase activity controls the molecular weight and polydispersity of polyhydroxybutyrate *in vivo*. Nat. Biotechnol. 15, 63–67.

Song, B.G., Kim, T.K., Jung, Y.M., Lee, Y.H., 2006. Modulation of talA gene in pentose phosphate pathway for overproduction of poly-beta-hydroxybutyrate in transformant *Escherichia coli* harboring phbCAB operon. J. Biosci. Bioeng. 102, 237–240.

Spiekermann, P., Rehm, B.H.A., Kalscheuer, R., Baumeister, D., Steinbuchel, A., 1999. A sensitive, viable-colony staining method using Nile red for direct screening of bacteria that accumulate polyhydroxyalkanoic acids and other lipid storage compounds. Arch. Microbiol. 171, 73–80.

Steinbuchel, A., Schlegel, H., 1991. Physiology and molecular genetics of poly(beta-hydroxy-alkanoic acid) synthesis in *Alcaligenes eutrophus*. Mol. Microbiol. 5, 535–542.

Tyo, K., Ajikumar, P., Stephanopoulos, G., 2009. Stabilized gene duplication enables long-term selection-free heterologous pathway expression. Nat. Biotechnol. 27, 760–765.

Tyo, K., Zhou, H., Stephanopoulos, G., 2006. High-throughput screen for poly-3-hydroxybutyrate in *Escherichia coli* and Synechocystis sp. Strain PCC 6803. Appl. Environ. Microbiol. 72, 3412–3417.

van Wegen, R.J., Lee, S.Y., Middelberg, A.P.J., 2001. Metabolic and kinetic analysis of poly(3-hydroxybutyrate) production by recombinant *Escherichia coli*. Biotechnol. Bioeng. 74, 70–80.

Wang, F., Lee, S.Y., 1997. Production of poly(3-hydroxybutyrate) by fed-batch culture of filamentation-suppressed recombinant *Escherichia coli*. Appl. Environ. Microbiol. 63, 4765–4769.

Wolfe, A.J., 2005. The acetate switch. Microbiol. Mol. Biol. Rev. 69, 12–50.